Supplement

Supplement S1 | Quantifying aboveground carbon density and its uncertainty

Correcting stem diameters for position of measurement

Stem diameters (D, in cm) are typically recorded at a height of 1.3 m aboveground. However, in some cases it may be necessary to measure D at a different point along the stem (e.g., in the presence of stem deformities or buttress roots). To account for differences in the position of measurement (POM, in m), we used the following taper model developed for Neotropical forests by Cushman *et al.* (2014) to reconstruct stem diameters at a height of 1.3 m aboveground ($D_{1.3m}$):

$$D_{1.3m} = \frac{D_{POM}}{\exp(-0.029 \times (POM - 1.3))} \tag{S1}$$

where D_{POM} is the stem diameter measurement taken at POM, which in in turn is expressed as a height in meters aboveground. When not reported, POM was assumed to be at 1.3 m aboveground.

Tree height estimation

Tree heights (H, in m) were measured for a subset of trees at Sepilok (n = 718), at Kuamut (n = 5587), in the SAFE experimental plots (n = 7653) and in the riparian buffer zones within the SAFE landscape (n = 1380), in the Global Ecosystem Monitoring (GEM) plots (n = 2769), and in both the CTSF plot and the CAO plots established at Danum Valley (n = 836 and n = 2769, respectively). In each case, H was measured using a laser range finder. Using these data, we developed site-specific H–D equations in order to estimate the height of trees that were not measured. Following the protocol outlined in the *BIOMASS* package in R (Rejou-Mechain et al., 2016), we compared a number of alternative H–D models with the intent of minimizing the residual standard error (σ) of the model. We found that a mixed-effects model of the form $\ln(H) = \rho_0 + \rho_1 \times \ln(D) + \rho_2 \times \ln(D)^2$, where ρ_{0-2} were allowed to vary by site (i.e., site was treated as a random effect influencing both the intercept and slope of the model), fit the data best (σ = 4.4; R^2 = 0.84). Fig. S1 illustrates the fit of this equation to the data.

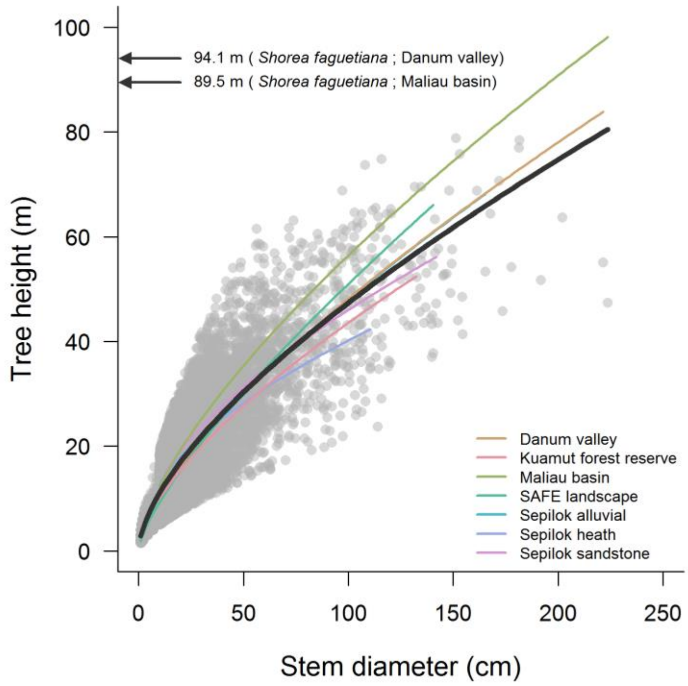

Fig. S1 | Relationship between tree height and stem diameter across study sites in Sabah. The black curve corresponds to the best fit *H–D* equation across all sites, while coloured lines illustrate how *H–D* relationships vary among sites. The height of the tallest known tree in Sabah (a 94.1 m tall *Shorea faguetiana* growing at Danum Valley, currently the tallest known tree in the tropics) and of the tallest tree at Maliau Basin (an 89.5 m tall *Shorea faguetiana*) are shown for context.

Wood density estimation

Wood density (*WD*, in g cm^{-3}) values were obtained from the Global Wood Density Database (Chave et al., 2009; Zanne et al., 2009). Prior to assigning *WD*, we first checked species names against those in the Taxonomic Name Resolution Service (Boyle et al., 2013). At Sepilok, in the CTSF plot at Danum Valley, in the GEM plots and in the CAO plots established at Danum Valley and Kuamut, trees were matched to species or closest taxonomic unit. If no taxonomic information was available, the mean *WD* of the plot was used instead (Talbot *et al.*, 2014; Rejou-Mechain *et al.*, 2016). For plots established as part of the SAFE forest fragmentation experiment and those in riparian buffer zones, trees were not identified taxonomically. In this case, *WD* values were assigned on the basis of disturbance history using data from the GEM plots as reference (see Table S1 for details).

Table S1 | Wood density (WD, in g cm^{-3}) values assigned to plots in the SAFE forest fragmentation experiment and in riparian buffer zones. For a description of the SAFE project, including the layout of the experimental blocks see Ewers *et al.* (2011). For a description of Global Ecosystem Monitoring (GEM) network plots see http://gem.tropicalforests.ox.ac.uk.

Site	Plot type	SAFE block	Disturbance history	GEM plot code	WD
Maliau	SAFE experiment	OG1, OG2, OG3	Old growth	Belian and Seraya	0.57
SAFE	SAFE experiment	VJR	Low logging intensity	Belian and Seraya	0.57
SAFE	SAFE experiment	LFE, LF1, LF2, LF3	Twice-logged continuous	LFE	0.61
SAFE	SAFE experiment	B	Twice-logged fragmented	B north and B south	0.46
SAFE	SAFE experiment	E	Twice-logged fragmented	E	0.53
SAFE	SAFE experiment	A, C, D, F	Twice-logged fragmented	E, B north and B south	0.48
SAFE	Riparian buffers	LFE	Twice-logged continuous	LFE	0.61
SAFE	Riparian buffers		Twice-logged fragmented	E, B north and B south	0.48

Accounting for missing stems in ACD and basal area estimation

With the exception of plots at Danum Valley and 38 of the SAFE experimental plots where all stems >1 cm in *D* were recorded, in other datasets compiled for this study the size threshold for inclusion was *D* = 10 cm. While large trees account for most of the biomass in forests (e.g., Bastin *et al.*, 2015), excluding small stems will nonetheless result in an underestimation of aboveground carbon density (*ACD*, in Mg C ha^{-1}), as well as basal area (*BA*, in m^2 ha^{-1}). To correct for this, we used the 45 1 ha plots at Danum to calculate *ACD* and *BA* using all available data (ACD_{1cm} and BA_{1cm}), and again after having excluded stems with *D* < 10 cm (ACD_{10cm} and BA_{10cm}). These data were then used to derive the following correction factors for *ACD* and *BA* which were applied to all other datasets (Fig. S2):

$$ACD_{1cm} = 6.713 + 1.004 \times ACD_{10cm} \tag{S2}$$

$$BA_{1cm} = 4.168 + 1.009 \times BA_{10cm} \tag{S3}$$

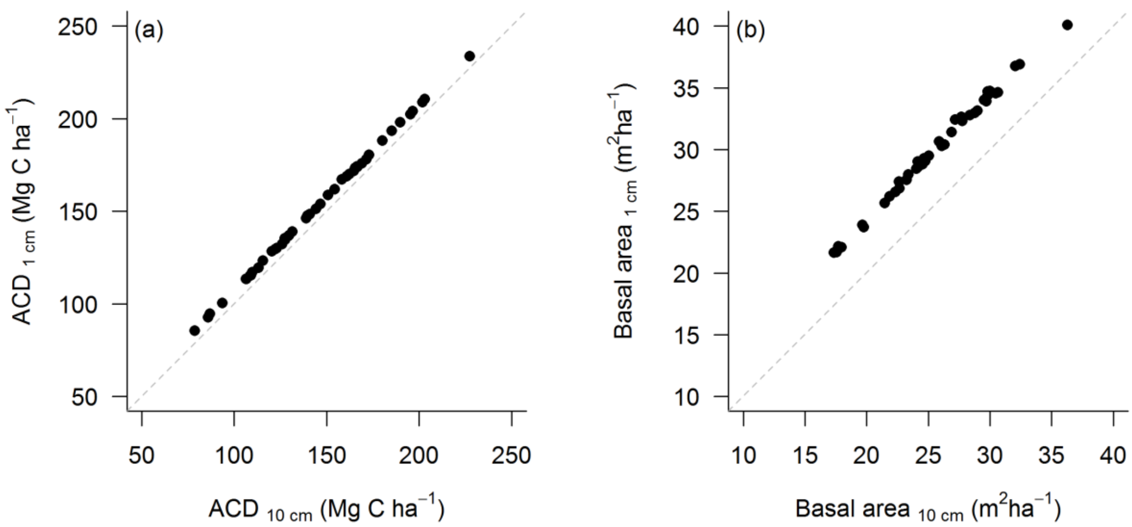

Fig. S2 | Relationship between (**a**) aboveground carbon density (*ACD*) and (**b**) basal area (*BA*) calculated with all stems > 1 cm in diameter (*D*) and after excluding stems with *D* < 10 cm for the 45 1 ha plots at Danum Valley. Dashed lines correspond to a 1:1 relationship.

Supplement S2 | Comparison of canopy metrics derived from NERC and CAO data

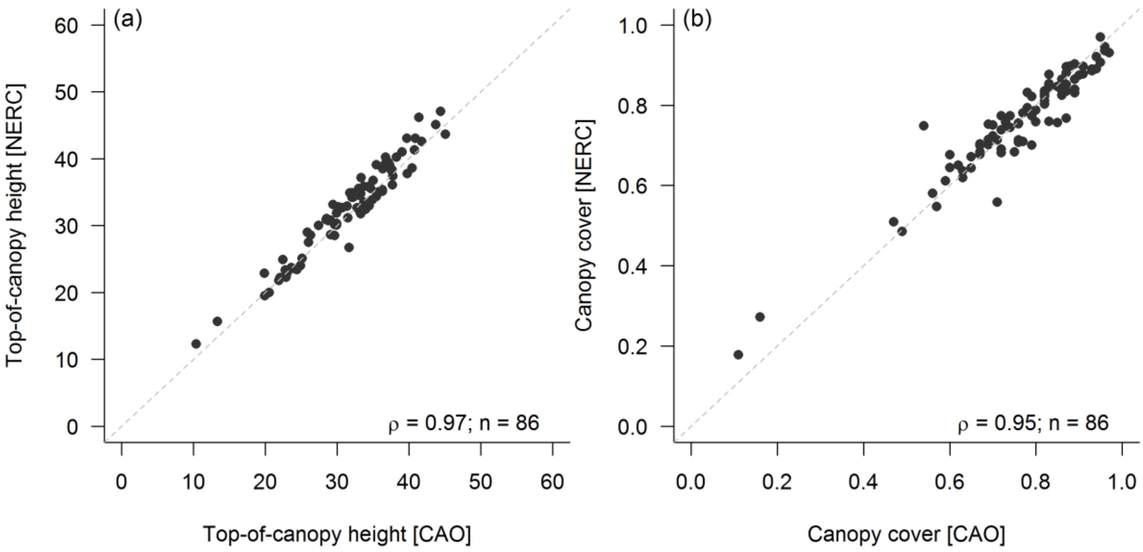

Fig. S3 | Comparison of (**a**) top-of-canopy height and (**b**) canopy cover at 20 m aboveground derived from NERC and CAO data. The comparisons are based on 86 field plots that were covered by both airborne campaigns. Note that a certain degree of departure from a 1:1 relationship (depicted by the dashed lines) is to be expected, as the two campaigns were flown more than 18 months apart across a region that is undergoing active logging and was affected by severe droughts associated with the El Niño event of 2015–16. Pearson's correlation coefficients (ρ) for each comparison are reported in the bottom right-hand corner of the panels.

Supplement S3 | Comparison of modelling approaches for estimating ACD

In addition to the aboveground carbon density (ACD) modelling approach described in the main text – which uses the L-BFGS-B nonlinear optimization routine to parameterize Eq. (4) and (6) – we compared two further modelling routines in an effort to identify the approach that would yield the lowest degree of systematic bias in the predicted values of ACD (see Table S2 in Supplement S4 below for a full list of equations referenced to here). The first relied on fitting a combination of ordinary and nonlinear least squares regression models to parametrise Eq. (2) and (4–7). These models did not account for potential spatial autocorrelation in the residuals, which could result in a slight underestimation of the true uncertainty in the fitted parameter values. We contrasted this approach with one that used generalised and nonlinear least squares regression that explicitly account for spatial dependencies in the data. In both case we found that these alternative modelling approaches substantially underperformed compared to the routine described in the main text. Both routines exhibited strong systematic bias in the predicted values of ACD, tending to substantially overestimate ACD for low carbon density forests and underestimate ACD in carbon rich ones (Fig. S4). This systematic bias in the model predictions was particularly evident in the case of the spatially explicit models (Fig. S4b).

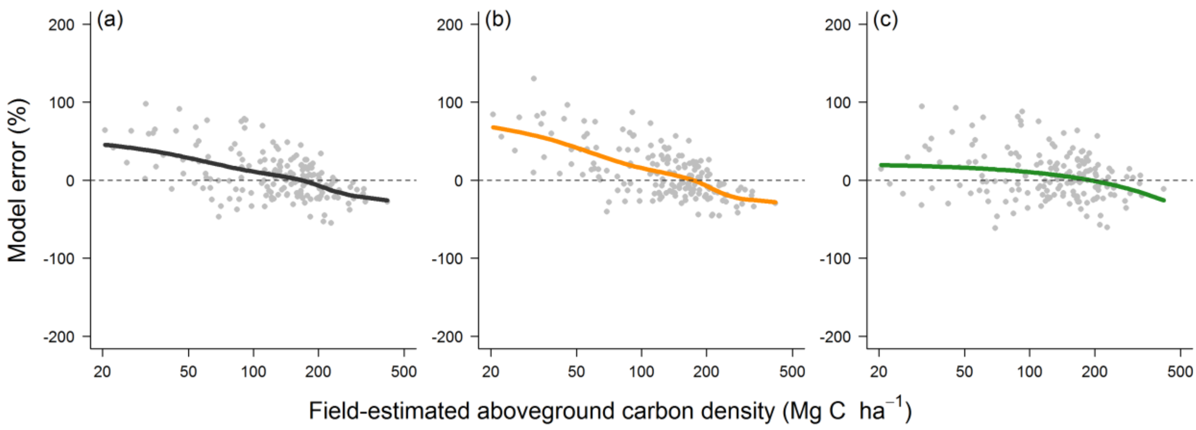

Fig. S4 | Comparison of mean relative model error (i.e., $\frac{ACD_{pred}-ACD_{obs}}{ACD_{obs}} \times 100$) as a function of field-estimated aboveground carbon density (ACD) for (**a**) models fit with a combination of ordinary and nonlinear least squares regression that do not account for spatial autocorrelation, (**b**) models fit with generalised and nonlinear least squares regression that explicitly account for spatial dependencies in the data and (**c**) the modelling routine descried in the main text. Each point corresponds to one of the 173 plots used to calibrate the models, while a regression spline fit to the data points is used to highlight systematic bias in model predictions.

Supplement S4 | Confidence intervals for parameter estimates

Table S2 | Parameter estimates for models presented in the main text. For Eq. (2), (3) and (6 – 7), best-fit parameter estimates are mean values across 100 model iterations, with 95% confidence intervals reflecting variation across all 100 model runs given in brackets. For each model, the equation number corresponds to that in the main text. σ is the residual standard error of the model.

Eq	**Model**	ρ_0	ρ_1	ρ_2	ρ_3	σ
2	$ACD = \rho_0 \times TCH^{\rho_1} \times BA^{\rho_2} \times WD^{\rho_3}$	0.567 [0.389; 0.829]	0.554 [0.452; 0.657]	1.081 [0.956; 1.213]	0.186 [-0.017; 0.351]	0.185
3	$BA = \rho_0 \times TCH$	1.112 [1.084; 1.142]				9.393
4	$ln\left(\frac{Cover_{20}}{1 - Cover_{20}}\right) = \rho_0 + \rho_1 \times ln(TCH)$	-12.431	4.061			0.101
6	$BA = \rho_0 \times TCH^{\rho_1} \times (1 + \rho_2 \times Cover_{resid})$	1.287 [1.217; 1.464]	0.987 [0.945; 1.000]	1.983 [1.904; 2.000]		6.581
7	$WD = \rho_0 \times TCH^{\rho_1}$	0.385 [0.279; 0.516]	0.097 [-0.013; 0.216]			0.225

Supplement S5 | Basal area and wood density predictions from ALS

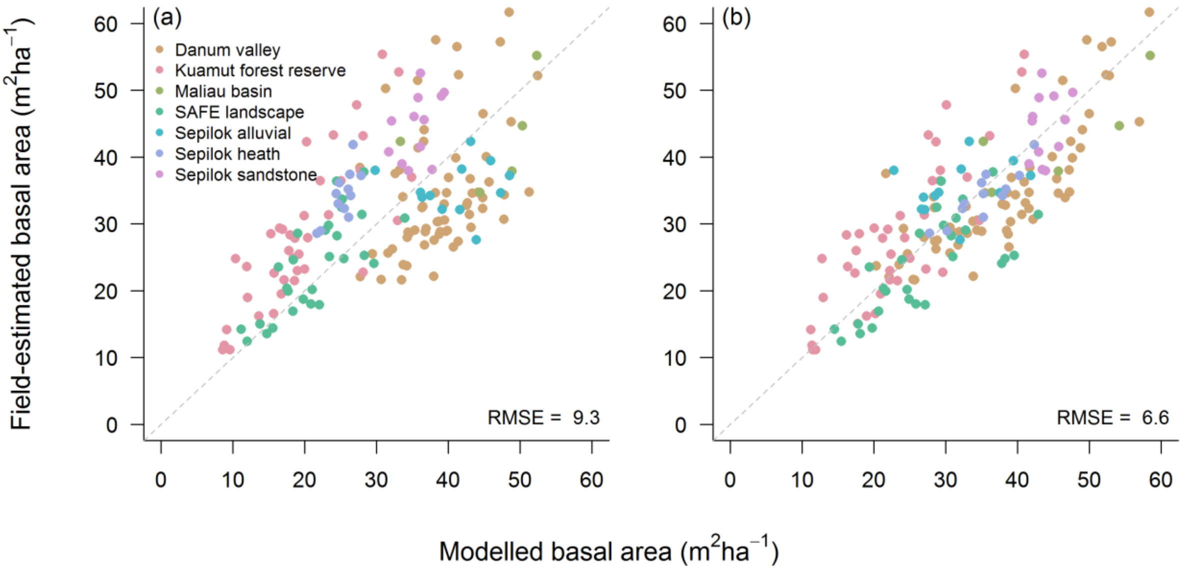

Fig. S5 | Relationship between field-estimated basal area (*BA*) and *BA* modelled as a function of (**a**) top-of-canopy height (*TCH*) [Eq. (9) in Table S2] and (**b**) a combination of *TCH* and canopy cover at 20 m aboveground [Eq. (10) in Table S2]. Dashed lines correspond to a 1:1 relationship. The RMSE of each comparison is printed in the bottom right-hand corner of the panels.

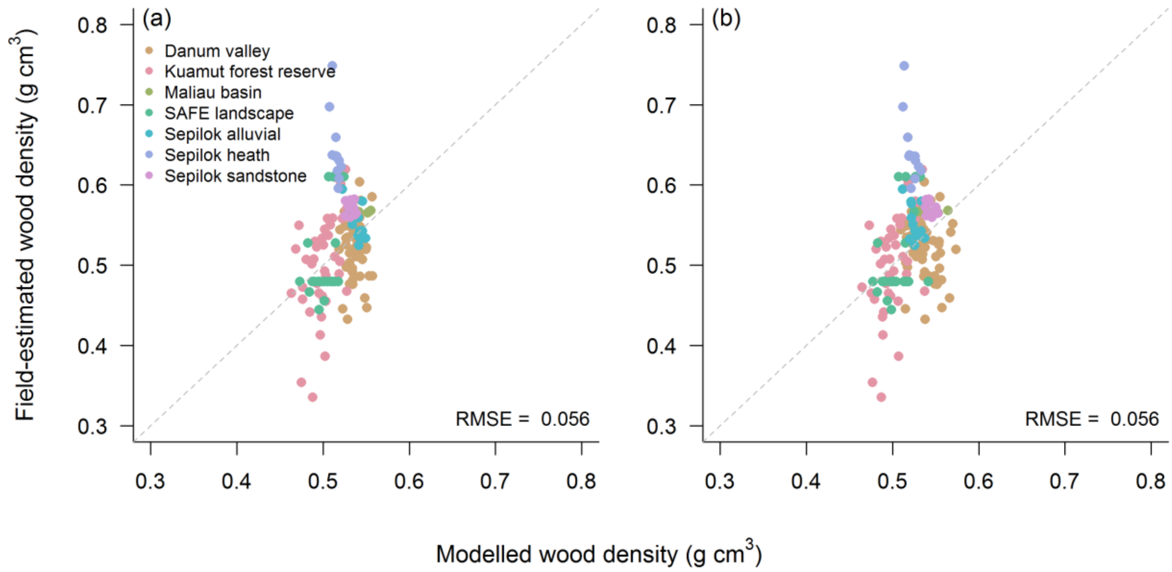

Fig. S6 | Relationship between field-estimated community-weighted mean wood density (*WD*) and *WD* modelled as a function of (**a**) top-of-canopy height [Eq. (11) in Table S2] and (**b**) canopy cover at 20 m aboveground. Dashed lines correspond to a 1:1 relationship. The RMSE of each comparison is printed in the bottom right-hand corner of the panels.

References

Bastin J-F, Barbier N, Réjou-Méchain M et al. (2015) Seeing Central African forests through their largest trees. *Scientific Reports*, **5**, 13156.

Boyle B, Hopkins N, Lu Z et al. (2013) The taxonomic name resolution service: an online tool for automated standardization of plant names. *BMC bioinformatics*, **14**, 16.

Chave J, Coomes DA, Jansen S, Lewis SL, Swenson NG, Zanne AE (2009) Towards a worldwide wood economics spectrum. *Ecology Letters*, **12**, 351–366.

Crawley MJ (2007) *The R book*. Wiley, Chichester, England.

Cushman KC, Muller-Landau HC, Condit RS, Hubbell SP (2014) Improving estimates of biomass change in buttressed trees using tree taper models. *Methods in Ecology and Evolution*, **5**, 573–582.

Ewers RM, Didham RK, Fahrig L, Ferraz G, Hector A, Holt RD, Turner EC (2011) A large-scale forest fragmentation experiment: the Stability of Altered Forest Ecosystems Project. *Philosophical Transactions of the Royal Society B*, **366**, 3292–3302.

Rejou-Mechain M, Tanguy A, Piponiot C, Chave J, Herault B (2016) *BIOMASS: Estimating above-ground biomass and its uncertainty in tropical forests*. R package version 1.0. https://CRAN.R-project.org/package=BIOMASS.

Talbot J, Lewis SL, Lopez-Gonzalez G et al. (2014) Methods to estimate aboveground wood productivity from long-term forest inventory plots. *Forest Ecology and Management*, **320**, 30–38.

Zanne AE, Lopez-Gonzalez G, Coomes DA et al. (2009) Global wood density database. *Dryad Digital Repository, http://dx.doi.org/10.5061/dryad.234*.